

Nano- and micro-scales structure and properties of the liquid-permeable piezoactive polyvinylidene fluoride films

I. S. Kuryndin, I. Yu. Dmitriev, V. K. Lavrentyev, N. N. Saprykina, G. K. Elyashevich

Institute of Macromolecular Compounds, Russian Academy of Sciences,
Bolshoy pr., 31, St. Petersburg, 199004, Russia

isk76@mail.ru, ivan-dmitriev-email@yandex.ru, lavrentev1949@mail.ru, elmic@hq.macro.ru, elya@hq.macro.ru

PACS 82.35.x, 61.41.+e

DOI 10.17586/2220-8054-2019-10-3-303-312

Liquid-permeable piezoactive polyvinylidene fluoride films were produced as porous membranes using preparation process including melt extrusion, annealing, cold/hot extension and poling consequent operations. The effect of technological control parameter at extrusion stage (melt draw ratio) on the characteristics of the film structure (overall porosity, liquid permeability and polymorphous composition) was investigated. The values of melt draw ratio which provides the permeability to liquids were established. The structure elements of nano- and micro- levels were determined by a number of experimental techniques. It was proved that the samples contain the pores with sizes 10 – 50 nm. The dependence of polymorphous composition and content of piezoactive crystalline modification on preparation conditions was analyzed. Permeable polyvinylidene fluoride films were successfully poled, and the stable piezoelectric response of the samples was demonstrated.

Keywords: polyvinylidene fluoride, porous films, permeability, structure scale levels, piezoelectric properties.

Received: 3 April 2019

Revised: 13 May 2019

1. Introduction

Polyvinylidene fluoride (PVDF) attracts great attention as a membrane material because it has several advantages for filtration and separation processes such as chemical and thermal stability, flexibility and mechanical strength [1–7]. PVDF films have been extensively applied in industrial sectors including environmental, electronic, energy, chemical and biotechnologies areas. However, fabrication of high performance PVDF materials remains challenging and has remained difficult to be achieved.

Permeable to liquids, porous PVDF films can be prepared using techniques based on the mechanism of phase inversion and thermally induced phase separation [4, 8, 9]. In these methods, the pores are generated by the extraction of a solvent. Extraction is carried out as the solution is evaporated, and a solid porous film is formed. By controlling the morphology, it is possible to produce PVDF films with various pore sizes and permeability. A mean pore diameter in the range of 20 – 100 nm was reported for such materials. Membrane production based on the phase separation method has two main drawbacks: solvent contamination and expensive solvent recovery.

Permeable films of semicrystalline polymers may be produced by a so-called “dry method” which is less expensive, more productive and reduces the environmental impact because no solvents (as a rule, they are generally toxic ones) are needed [10–12]. This technique is based on the extension of a film containing a highly oriented stacked lamellar structure. It has been successfully employed for fabricating microporous polypropylene and polyethylene microporous films. There are three consecutive stages of the process: (1) melt extrusion to produce the precursor film with an oriented lamellar morphology, (2) annealing of this film to thicken the lamellae due to involving of macromolecular chains from amorphous regions into the crystals, and (3) uniaxial extension of the film at room temperature to create voids between lamellae, and then thermal stabilization of the porous structure. Stage (1) is a complex process because the film should be produced under high melt draw ratios and cooling rates. Stages (1) and (2) provide the specific morphology formed by stacks of flat lamellar crystallites arranged perpendicularly to the orientation direction of the macromolecular chains. Due to this structure, the effective pore creation is possible as a result of lamellae separation during extension at stage (3). It was proved that the 3-step process (melt extrusion–annealing–uniaxial extension) gives the possibility to obtain microporous PVDF films [13–17]. The porous structure of the PVDF membranes containing open to the surface and closed in the volume pores and permeable for water vapor have been produced [16]. At the same time, liquid-permeable PVDF membranes produced by melt extrusion technology haven't been reported to the best of our knowledge.

It should be noted, that PVDF is widely used not only in the membrane industry but also as the most common non-ceramic piezoelectric material in the electrical industry [18, 19]. Recently, it was shown [20–23] that electrical excitation of the piezoelectrically vibrating membranes (as PVDF, as inorganic piezomembranes, both) could increase

the flux and markedly reduce membrane fouling. The results of the filtration experiments of Darestani [20, 21] using the piezoelectric PVDF materials showed that the vibrations delayed membrane fouling significantly while the membrane flux was maintained close to its initial value. Another innovating point is design of oscillatory resonant devices for gravimetric biosensors (microbalances) based on porous PVDF piezofilms as an alternative for piezoelectric quartz crystals [24]. A new concept was also introduced for self-charging power cells (piezocapacitors) based on piezoactive PVDF separators, in which the mechanical energy is directly converted into electrochemical energy through a piezoelectric effect and is directly stored in a Li-ion battery [25–27]. All of these investigations involve the use of porous piezoactive PVDF films, therefore elaboration of new synthetic approaches seems relevant.

PVDF is a crystallising polymer, and it has at least four crystalline modifications (α , α_c , β and γ) [28]. The all-trans β -phase is ferroelectric and mainly responsible for its piezoelectric properties. At the same time, melt processing techniques yield only α -phase and the polymorphic transition from α - to β -modification can be efficiently implemented using the orientation drawing at temperatures between 60 and 90 °C or under increased pressure [28, 29]. Therefore, the development of an approach that enables the formation of piezoactive β -crystallites in porous PVDF materials is an important task for practical application of PVDF.

It is important to note that for transformation of PVDF films into a piezoelectrically active state an electrical poling must be carried out. Poling involves the application of an electric field at elevated temperatures to orient the polar axis of the β -phase domains in the field direction. This allows alignment of the β -phase crystals and converts an inactive β -PVDF film into an electromechanically active material. In order to achieve a large piezoelectric response in PVDF materials, the poling process usually requires an external field of higher than 30 MV/m at temperatures of 70 – 100 °C. Poling can also result in partly conversion of the α -phase to the β -phase [28]. However, there is the technological obstacle to polish porous structures because the voids are able to promote breakdown [29, 30]. To overcome this difficulty, the special method was elaborated. As an electrode the common aluminium adhesive tape was used. A thin adhesive layer played the role of an additional insulator protecting from electrical breakdown. The advantage of this approach is in its simplicity. Aluminium adhesive tapes provide satisfactory DC poling of PVDF at increased temperature and can be easily peeled off after the poling, and porous structure is not damaged. A poled porous film is a ready to use piezoactive membrane.

A liquid metal (eutectic gallium–indium–tin alloy) was used as an electrode for piezoelectric modulus measuring in this work. It can be easily rubbed in the surface of the PVDF porous films without permeation inside them. The liquid metal can be easily erased from the surface of the porous film. Thus, the proposed method of the poling technique is a universal approach which gives an opportunity to produce the materials with stable piezoelectric response. Specific applications of this approach may lay in the field where large-area piezoactive films are needed (much more than 10 cm²). The applicability of “dry method” for through porous PVDF films preparation and their piezoelectric performance has not been investigated yet to the full extent.

The applicability of “dry method” for through porous PVDF films preparation and their piezoelectric performance has not been investigated yet to the full extent. The goal of this study was to obtain the porous liquid-permeable and, at the same time, having piezoactive PVDF films in the process including the stages of melt extrusion/annealing/extension/poling and determine the permeability, porous structure characteristics, content of piezoactive β -crystallite modification and piezoelectric modulus.

The goal of this study was as follows:

- to obtain the porous liquid-permeable and, at the same time, piezoactive PVDF films using a melt extrusion process;
- to perform poling of these films by electric voltage;
- to determine the porous structure characteristics, content of piezoactive β -crystallite modification and piezoelectric modulus.

2. Materials and Methods

Commercial PVDF grades Kynar 720 (Atofina Chemicals Inc., USA) with melt index 10 g/10 min (230 °C, 5 kg) and melting temperature 168 °C were used. The PVDF films were formed on a laboratory single screw extruder (Scamia, France) with a slit die. Two processing parameters were controlled at this stage: die gap and extruder screw speed. Other parameters such as uptake speed (3.2 meters per minute) and melt extrusion temperature (die temperature 200 °C) were kept constant. The melt draw ratio was varied by adjusting of screw speed and die gap (Table 1) and calculated as:

$$\lambda = S \cdot \rho \cdot l / m,$$

where S – the die gap area (cm²), ρ – density of the extruded film (1.78 g·cm⁻³), m and l – weight (g) and length (cm) of the extruded film piece. In this work λ was varied from 55 to 157 (Table 1).

TABLE 1. The effect of extrusion parameters on characteristics of the extruded PVDF films

Die gap, mm	Screw speed, s ⁻¹	Melt draw ratio	Thickness, μm
1.0	0.75	55	22
1.0	0.50	84	15
1.5	0.75	103	18
1.5	0.50	157	12

The extruded films were annealed under isometric conditions (at fixed ends of the sample to avoid the shrinkage of an oriented film at heating) during 1 h at a temperature near the melting point of the polymer (167 °C). The uniaxial extension of the annealed films was carried out in air in the orientation direction at a velocity of 40 mm/min. The first (“cold”) extension was carried out at room temperature up to 40 % elongation. However, cold drawing alone leads to the formation of porous structure, permeable to vapors and gases but not permeable to liquids because it has low porosity and does not contain through flow channels. To enlarge the number and sizes of pores the second (“hot”) extension stage was carried out at 100 °C up to 50 %. After the “hot” extension, the films were subjected to thermal stabilization under isometric conditions for 1 h at 100 °C to prevent shrinkage after stress relief and to take off the inner stress initiated by orientation.

The stress–strain curves were obtained at uniaxial extension of the annealed samples with sizes 5 × 50 mm at the rate 50 mm·min⁻¹ in a 2166 R-5 tensile test machine (Tochpribor, Russia). The stress-strain curves were used to determine yield stress, breaking strength, elastic modulus and break elongation. For each sample no less than five measurements were performed. The measurement error calculated as the standard deviation did not exceed 10 % of the average value of the determined characteristic. The annealed films were characterized by the value of elastic recovery ER_{50} which was measured at cyclic loading of the samples up to extension 50 % at velocity 50 %·min⁻¹. ER_{50} was calculated in percents as ratio of recovery deformation of the sample to its total deformation at the first cycle.

The overall porosity of the samples was calculated by the Eq.:

$$P = [(\rho - \rho_p) / \rho] \times 100 \%,$$

where ρ_p is the density of the porous film, which was measured gravimetrically.

The permeability of the porous films to liquids was estimated by filtration porosimetry based on the flow of a liquid through the PVDF sample. This method is a nondestructive one and, in addition, it is similar to the operation conditions under which microfiltration membranes are usually used. Permeability measurement was performed in a filtration cell under a pressure of 0.5 MPa. Ethanol was used as a wetting liquid in the experiment. To measure the permeability of water, which is nonwetting liquid for PVDF, it was necessary previously to wet the sample previously by ethanol and then to flow water through the sample. The permeability value is inversely to liquid viscosity. Viscosities of ethanol and water at 20 °C are 1.197 and 1.006 mPa/s, respectively. It was tested that permeability to water is on 15 % higher than to ethanol for all porous samples.

The wide-angle X-ray scattering studies were performed using a DRON 2.0 diffractometer (Burevestnik, Russia) with CuK α radiation. Recording was carried out in a transmission mode. To determine the degree of orientation of the samples, azimuthal curves of intensity of reflection (110) were obtained. The degree of orientation was estimated by calculating the orientation factor through the following Eq. [31]:

$$f_c = \frac{3 \langle \cos^2 \varphi \rangle - 1}{2},$$

where φ is the angle between the extrusion direction and the crystalline chain axis.

It is known that, as a rule, the crystalline structure of PVDF samples contains the mixtures of polymorphous modifications, mainly, α and β crystals. To characterize the sample, it is necessary to determine the portions of these crystalline phases. At the same time, the structural methods such as Infrared Spectroscopy (IR) and Differential Scanning Calorimetry (DSC) cannot be used to determine the percentage of crystalline phases in PVDF films: the IR spectra permit to characterize these phases qualitatively but not quantitatively because of difficulties in peaks resolution [28]. The same can be said about melting peaks on DSC. In the previous works (for example, 16, 17, 28), X-ray scattering was used to identify the crystalline phases in PVDF by recording the equatorial reflections located in the vicinity of $2\theta = 20^\circ, 17.66^\circ, 18.30^\circ, 26.56^\circ$ for α - and 20.26° for β - phases, respectively. It was shown that the diffraction peaks for the phases partially overlap with each other, and therefore, it is impossible to separate correctly

these reflections. In the present work, the meridian reflections disposed at 39° and 35° for α - and β - modifications [32], respectively, were recorded in the orientation direction of the film in transmission mode to estimate quantitatively the content of these crystalline phases.

The degree of crystallinity was determined by the Hermans–Weidinger method [31] using the samples prepared by stacking of randomly oriented pieces of the porous films. The thickness of lamellae was determined by the half-width of the meridional reflex using the Debae–Scherrer formula. In earlier work [15] we measured thickness of lamellae in the extruded and annealed samples by small-angle X-ray scattering, and the values obtained by these methods differ by no more than 10 – 20 %. Thickness of lamellae in the samples formed at the extrusion and subsequent annealing was measured by small-angle X-ray scattering [15].

The porous structure parameters were calculated from the N₂ adsorption/desorption isotherms, which were obtained using Surface area analyzer “Sorbometr-M” (Katakon, Russia). The standard sample holder was loaded with pieces of the porous film with the total mass 0.15 – 0.25 g. The samples specific surface area was estimated from the Brunauer–Emmett–Teller (BET) model. The pore size distribution was obtained using the isotherm measured over the relative pressure range of (P_s/P_o) from 0.30 to 0.99.

The surface and cross-section morphology of the samples were studied using scanning electron microscopy ZEISS MERLIN (Germany) at the voltage of 10 kV. Film cleavages were obtained by the brittle failure technique in liquid nitrogen.

The PVDF porous films were poled by a contact method of thermal poling. Aluminum adhesive tape was used as an electrode material. For electrical poling, metalized PVDF membrane was sandwiched between two electrodes in the poling setup which was set in a thermostat at 90 °C. The voltage between the electrodes was increased step-wise from zero to 105 V· μm^{-1} at a rate of 50 V·min⁻¹. A DC power supply B5-24A (Russia) was used to generate the desired electric potential difference. After that, the film was cooled to room temperature under the electric field. The experiment was repeated at least three times for each sample.

After the sample poling, the aluminum adhesive tape was carefully removed from the film, the surfaces was thoroughly cleaned by ethanol and metalized again with a liquid metal (eutectic gallium–indium–tin alloy) which was applied on the sample surface manually. The reason for the second metallization is that the adhesive conductive tapes don't allow registering the piezoresponse because of isolating action of a thin glue layer. To the contrary, the liquid metal can't be used for thermal polarization of permeable membranes because of increased probability of breakdown as a result of metal penetration into the through channels. The thin isolation glue layer of the aluminum adhesion tape acts as a breakdown protector for porous film polarization, but it has to be substituted for an appropriate contact electrode layer after the poling procedure.

Transverse piezoelectric coefficient d_{31} was measured by static tension applied to the polarized films with the liquid metal contacts along the orientation axis. Mechanical stress of the sample was set from 5 to 20 N (12 – 40 MPa). The potential difference at the contact electrodes of the sample at its deformation was measured using a R-30 potentiostat (Elins, Russia). Piezoelectric coefficient d_{31} was calculated by equation [34]:

$$d_{31} = \frac{C \cdot \Delta U \cdot B}{A \cdot \Delta F},$$

where C is the sum of capacities of the sample and a reference capacitor (1 μF), A is area of the electrodes on the sample surfaces (cm²), B is the cross-section area of the film (cm²), ΔU is the voltage values (V), and F is an applied tensile force (N).

3. Results and discussion

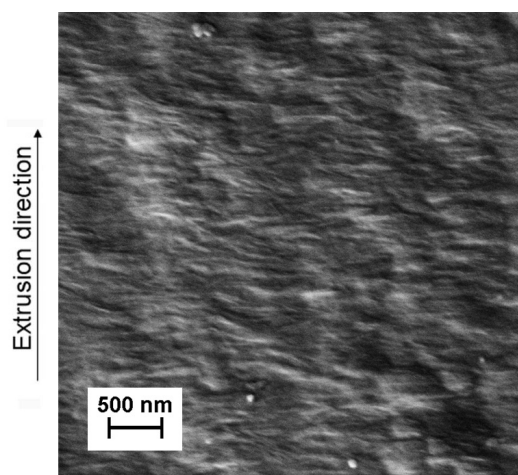
3.1. Characterization of the extruded and annealed PVDF films

Due to melt drawing, the samples formed at extrusion stage have the oriented structure, and the orientation degree is determined by melt draw ratio λ (Table 2). This is displayed in the pictures of scanning electron microscopy (SEM) (Fig. 1), where the surface images of PVDF extruded films exhibits highly oriented lamellar stack morphology. It is known [10, 14, 15] that this structure is the most suitable for pores formation in the process of subsequent uniaxial extension which initiates moving apart of lamellae and appearance discontinuities between them. It was shown by X-ray data that the sizes of lamellae in PVDF extruded films were as 7 – 8 nm. These is values does not depend on λ because it is determined by crystallization temperature of the extruded films which was constant in the process of their solidification during film formation procedure.

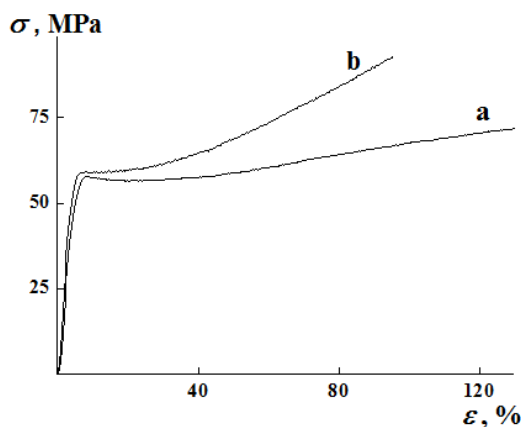
Isometric annealing of the extruded films at high temperature close to PVDF melting point is the important stage which makes it possible to enlarge orientation degree (annealing is carried out at the stress provided by fixation of the film ends) and also to increase considerably the thickness of lamellae which reaches 11 – 12 nm. As it can be seen from Table 2, the orientation factor of the annealed films increases from 0.90 to 0.97 as λ grows from 55 to 157.

TABLE 2. Orientation degree and mechanical characteristics of the annealed PVDF films

λ	f_c	Yield stress, MPa	Breaking strength, MPa	Young's modulus, MPa	Elongation at break, %	Elastic recovery, %
55	0.90	58	75	1460	130	71
84	0.93	59	81	1520	114	81
103	0.94	59	86	1570	94	87
157	0.97	60	98	1680	71	89

FIG. 1. SEM picture of surface for the extruded PVDF films formed at $\lambda = 55$

Mechanical characteristics of the annealed films are also found to be dependent on melt draw ratio (Fig. 2). Breaking strength and elastic modulus increase with growth of λ (Table 2). At the same time, elongation at break decreases with increasing of λ that indicates a rising of their hardness.

FIG. 2. Stress-strain curves for annealed samples with $\lambda = 55$ (a) and 103 (b)

Stress-strain curves analysis of the annealed PVDF films is useful for understanding of porous structure formation under uniaxial extension of the annealed samples (Fig. 2). The initial linear part of the stress-strain curves characterizes the elastic deformation of the samples up to the yield stress point. Yield stress is well pronounced for $\lambda = 55$ but less and less observed for the samples as λ grows. In the second part of the curve, following an intermediate region, an almost linear increase in the stress (strain hardening) is observed. This increase is responsible for the elastic character of the lamellar deformation and growth of number and size of the pores. Fig. 2 demonstrates that the higher melt draw

ratio is the less pronounced the yield stress becomes, the higher the rupture strain and the more stronger the second slope which is responsible for the lamellar deformation. Thus at increasing of λ the annealed samples acquire “hard elastic” properties, namely, capability to large elastic reversible deformations. The cyclic loading (Fig. 3) demonstrates the “hard elasticity” of the annealed samples which were characterized by the value of elastic recovery ER_{50} as ratio of reversible deformation to total one. It is seen in Table 2 that ER_{50} increases with λ . It was shown [10,35] that hard elastic properties are the necessary condition for porous structure formation at subsequent extension.

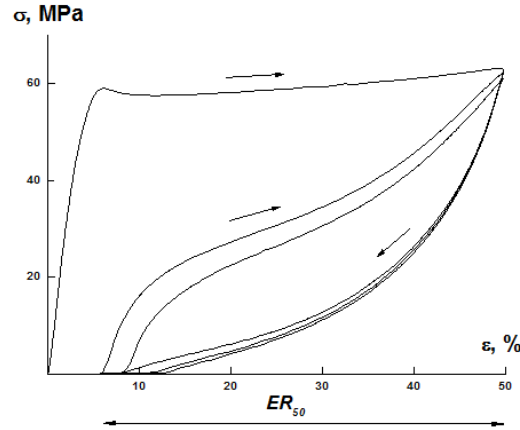


FIG. 3. Stressstrain curves for the annealed film with $\lambda = 103$ under cyclic loading

3.2. Structure of the PVDF porous films

The influence of melt draw ratio on the structure of the porous PVDF films obtained by two-step – “cold” and then “hot” – uniaxial extension (40 and 50 %, respectively) is shown in Table 3. As it can be seen, the overall porosity of the film formed at $\lambda = 55$ is 21 % while for the samples obtained at $\lambda = 84 - 157$, it reaches 26 – 28 %. According to the measurements by filtration porosimetry, the film prepared at $\lambda = 55$ is impermeable while the samples extruded at $\lambda = 84 - 157$ are permeable that is the evidence that these films contain through flow channels connecting two surfaces of the film providing them with through permeability. Thus, it can be concluded that the percolation threshold to reach the through permeability is found to lie around 25 % overall porosity that approximately corresponds to $\lambda \sim 60 - 70$. This result is in accordance with the porosity percolation threshold determined by percolation theory as 25 – 30 % [36]. It was confirmed for PE and PP porous films obtained by the same (“dry”) method [10, 35].

TABLE 3. Structure characteristics of PVDF porous films

Melt draw ratio	$\lambda = 55$	$\lambda = 84$	$\lambda = 103$	$\lambda = 157$
Thickness, μm	19	13	16	11
Overall porosity, %	21	26	27	28
Liquid permeability (ethanol), $\text{l}\cdot\text{m}^{-2}\cdot\text{h}^{-1}\cdot\text{atm}^{-1}$	Impermeable	1.1	0.9	1.3
Liquid permeability (water), $\text{l}\cdot\text{m}^{-2}\cdot\text{h}^{-1}\cdot\text{atm}^{-1}$	Impermeable	1.3	1.1	1.5
Degree of crystallinity, %	58	60	61	63
Content of β -phase, %	38	31	20	15

It is seen in Table 3 that film permeability grows with increasing of λ and with decreasing of the die gap. This allows one to conclude that the optimal morphology for the effective through pores appearance at the stage of uniaxial extension is formed at the extrusion stage in the range of $\lambda > 60 - 70$.

Crystalline structure of the porous films was investigated by X-ray diffraction. According to the calculations of intensities of the meridional X-ray reflections, the crystalline phase of the extruded and annealed samples consists of

α -modification alone. It was found that all the microporous PVDF films contain a mixture of α - and β -crystallites (Table 3 and Fig. 4).

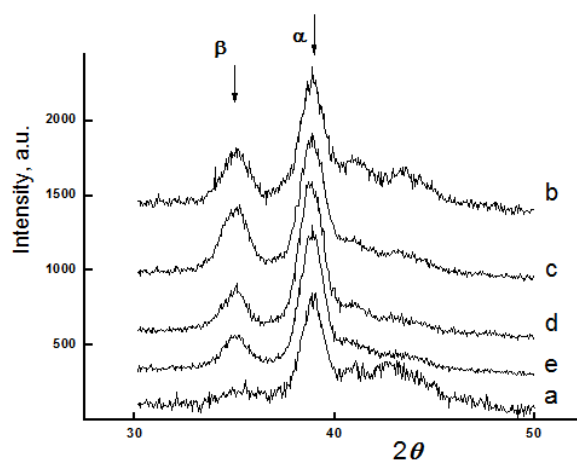


FIG. 4. Meridional X-ray diffractograms of the annealed (a) and porous PVDF films with $\lambda = 55$ (b), 84 (c), 103 (d) and 157 (e)

In this preparation technique the porous structure formation and also $\alpha > \beta$ -transition, both, are initiated by the uniaxial extension of the annealed PVDF films. Note that the data given in Table 3 demonstrates that the percentage of β -phase decreases with increasing of melt draw ratio. It may be explained by the fact that at lower orientation at the extrusion stage, the less perfect, weakly oriented crystals are formed (as compared with ones formed at higher λ), and consequently it is easier to implement $\alpha > \beta$ -transition on the subsequent uniaxial extension stage. At the same time, it was established in [29] that an increasing of orientation degree at extension leads to the growth of β -phase content for the films extruded at all λ .

3.3. Morphology of the porous PVDF films

The results of SEM investigations of the porous samples are presented at Fig. 5. The surface of the impermeable film ($\lambda = 55$, Fig. 5(a)) is filled with dense solidified structure elements, connected by fibrils. The surface structure is weakly oriented and has few ruptures (pores). In contrast, the permeable films surface ($\lambda = 103, 157$, Fig. 5(b,c)) has greater porosity and disrupted fibril-like ties inside the pores. This clearly illustrates the fact that at the extension of the annealed films obtained at the highest value of λ the mechanical stress leads to lamellar separation but not to reorientation, spherulites splitting and etc.

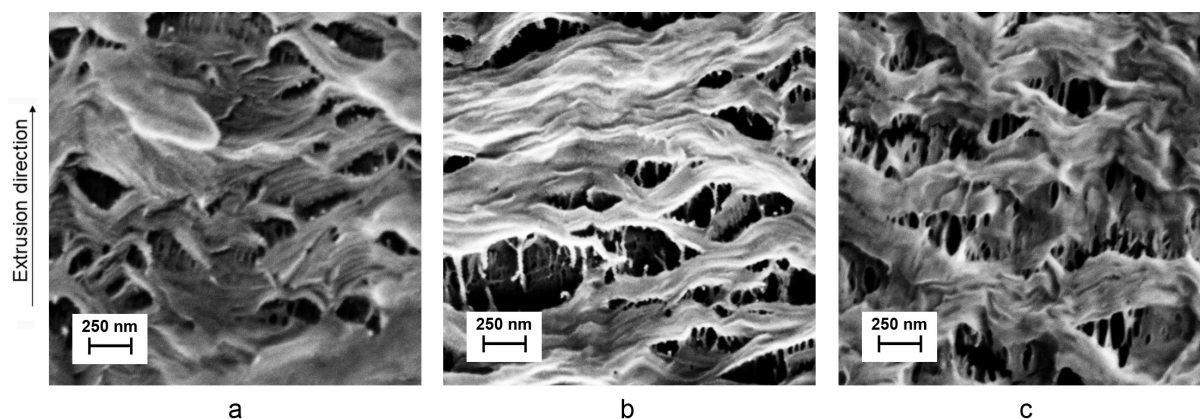


FIG. 5. SEM micrographs of surface of the PVDF porous films with $\lambda = 55$ (a), 103 (b), 157 (c)

The denser structure with smaller pores can be noticed beneath the large, opened to surface pores (Fig. 5(b)). Electron microscopy of the porous films cross-section shows that the scale of surface structure elements differs from inner regions ones (Fig. 6). As it can be seen at Fig. 6, the morphology of the surface is characterized by the large

wavy structures which have a scale relief in submicro- and micrometer range $0.1 - 1.0 \mu\text{m}$. In contrast, in the inner part of the sample there are the smaller scale pores with the sizes less 50 nm located in the inter-lamellar regions (Fig. 6).

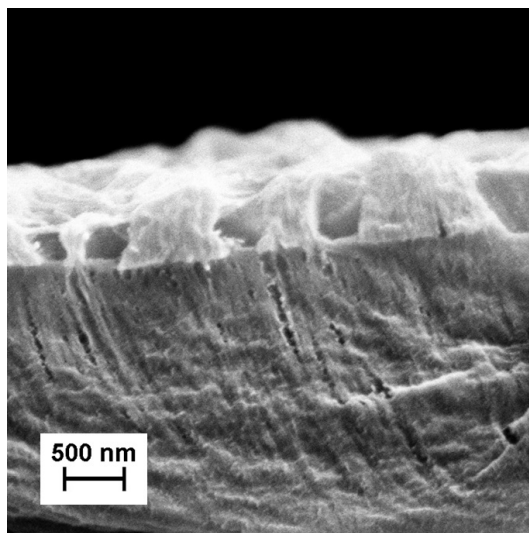


FIG. 6. SEM micrographs of cross-section of the permeable PVDF film ($\lambda = 103$)

Highly developed surface relief (Figs. 5–6) of the prepared porous films are able to produce a high specific surface area. Low-temperature gas adsorption method (method BET) gave specific surface of the permeable samples about $37 \text{ m}^2 \cdot \text{g}^{-1}$. Note that nonporous extruded and annealed films have specific surface in order $10^{-3} \text{ m}^2 \cdot \text{g}^{-1}$. The pores size distributions have a maximum in the range of diameters $10 - 30 \text{ nm}$ (Fig. 7). Increasing of λ leads to a few shift of maximum of the curve to the larger sizes (at 5 nm), and also to the growth of volume of pore space, i.e. number of pores. This provides evidence that the sizes $10 - 50 \text{ nm}$ is a characteristic structural parameter for this system, and an increase in the permeability with orientation degree is mainly due to rising in the number of pores. It should be noted, that the pore size distribution calculated from adsorption isotherm (method Barrett–Joyner–Halenda) is in accordance with the SEM data of the sample cross-sections where the pores about $15 - 50 \text{ nm}$ can be visually estimated (Fig. 6).

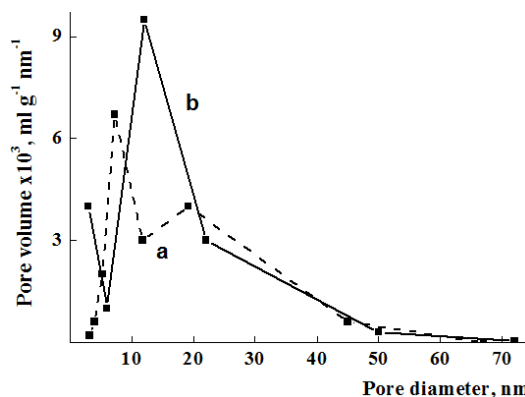


FIG. 7. Pores size distributions of the permeable porous PVDF film formed at $\lambda = 55$ (a) and 103 (b)

Thus, investigations of permeable PVDF porous films performed by a number of experimental techniques demonstrate the complicated structure consisting of elements of different scale levels: surface relief is formed by structure details of micrometer scale, the sizes of pores are in the range of several tens of nanometers, and, at last, crystalline lamellae have the thickness of about 10 nm . However, the design of structure on the surface and inside the porous samples has the similar character that allows us to classify the sample structure as fractal.

Maximal permeability which have been reached in this work (1.3 and $1.5 \text{ l} \cdot \text{m}^{-2} \cdot \text{h}^{-1} \cdot \text{atm}^{-1}$ for flowing of ethanol and water, respectively) is rather small as compared with the PVDF films obtained by “wet method” which have the

larger pore sizes (50 – 300 nm) than our samples (Fig. 7). But the “wet method” process produces the membranes which are characterized by much wider pore size distribution, i.e. by low separation selectivity. And also, it is important to note, that “dry” technology is based on solvent-free and cost effective process comprising melt extrusion, thermal and mechanical treatments. Moreover, PVDF porous films prepared in this work have the additional functionality, namely, they demonstrate piezoactive properties.

3.4. Poling and stability of piezoelectric characteristics

To characterize the piezoelectric properties in porous PVDF films, the DC poling was performed for the impermeable ($\lambda = 55$) and permeable ($\lambda = 84$) ones. These samples possess the similar values of crystallinity but they have the different porosity and β -phase content (Table 3). It was found (Table 4) that the values of piezomodulus along the sample orientation (d_{31}) are close to each other (10 – 11 pC·N⁻¹) but have a tendency to decrease for the sample with lower content of piezoactive component. After the first month of storage at ambient conditions, the films’ piezoelectric modulus decreased by $\sim 15\%$ and 27% for impermeable and permeable samples, respectively. However after the next month of storage, both samples showed a high stability of polarization over time (Table 4). Note that the poling does not induce decreasing of permeability of the samples, which remains on the same level as it was before high voltage application (1.1 l·m⁻²·h⁻¹·atm⁻¹).

TABLE 4. Piezomodulus d_{31} (pC·N⁻¹) of the microporous PVDF films with $\lambda = 55$ and 84

Storage time	$\lambda = 55$ (impermeable)	$\lambda = 84$ (permeable)
Immediately after polarization	11.5	10.4
After 1 month	9.7	7.6
After 2 month	9.5	7.5

Thus, in this work, for the first time, for PVDF membranes were prepared by the a “dry method” the that attained both liquid permeability and piezoelectric response, both, are reached. These films may be used for electrically controlled systems design (piezosupercapacitors, piezobiosensors, oscillating fouling-resisted membranes and etc.).

4. Conclusions

Porous PVDF films which combine through permeability and also piezoactivity were successfully produced in the effective, ecologically safe manufacturing process based on polymer melt extrusion. The effect of melt draw ratio on the overall porosity and liquid permeability was investigated in this paper for the first time. Optimal operating parameters for melt extrusion were determined for successful pores nucleation and growth to reach the percolation threshold for the appearance of liquid permeability. The permeable membranes were obtained when extrusion process was performed at melt draw ratios higher than 60 – 70 which corresponds to the percolation threshold for overall porosity 23 %. At the higher melt draw ratios the permeability increases, but the overall porosity does not change. It was found that the films contained the pores with sizes 15 – 50 nm. The surfaces of the films were found to have a strongly developed relief with scale of relief in order 1 – 2 μ m. The content of β -phase in the permeable films having piezoproperties reaches more than 30 %. Hierarchy of structure elements on micro- and nano-scale levels have been investigated, and the possibility to regulate the characteristics of the samples by processing parameter at extrusion stage of the preparation process to reach the desired combination of properties was demonstrated. Also, new possibilities of poling were revealed for the permeable to liquids PVDF films which were successfully poled, and stable piezoelectric response was demonstrated. The “dry method” of porous PVDF piezoactive membranes preparation presented herein stimulates further research because the unique combination of their properties are of outstanding interest for a number of application fields such as membrane technology, storage, conversion and harvesting of energy.

References

- [1] Davenport D.M., Gui M., Ormsbee L.R., Bhattacharyya D. Development of PVDF Membrane Nanocomposites via Various Functionalization Approaches for Environmental Applications. *Polymers*, 2016, **8** (32).
- [2] Ji J., Liu F., Hashim N.A., Abed M.R.M., Li K. Poly(vinylidene fluoride) (PVDF) membranes for fluid separation. *Reactive & Functional Polymers*, 2015, **86**, P. 134–153.
- [3] Kang G., Cao Y. Application and modification of poly(vinylidene fluoride) (PVDF) membranes – A review. *Journal of Membrane Science*, 2014, **463**, P. 145–165.

- [4] Liu F., Hashim N.A., et al. Progress in the production and modification of PVDF membranes. *Journal of Membrane Science*, 2011, **375**(1–2), P. 1–27.
- [5] Lai Ch.Y., Groth A., Gray S., Duke M. Nanocomposites for Improved Physical Durability of Porous PVDF Membranes. *Membranes*, 2014, **4** (1), P. 55–78.
- [6] Zhang Q., Lu X., Zhao L. Preparation of Polyvinylidene Fluoride (PVDF) Hollow Fiber Hemodialysis Membranes. *Membranes*, 2014, **4** (1), P. 81–95.
- [7] Liu F., Xu Y.Y., et al. Preparation of hydrophilic and fouling resistant poly(vinylidene fluoride) hollow fiber membranes. *Journal of Membrane Science*, 2009, **345** (1–2), P. 331–339.
- [8] Kima J.F., Jung J.T., et al. Microporous PVDF membranes via thermally induced phase separation (TIPS) and stretching methods. *Journal of Membrane Science*, 2016, **509**, P. 94–104.
- [9] Cui Z.Yu., Xu Y.Y., et al. Preparation of PVDF/PMMA blend microporous membranes for lithium ion batteries via thermally induced phase separation process. *Materials Letters*, 2008, **62** (23), P. 3809–3811.
- [10] Kuryndin I.S., Lavrentyev V.K., Bukoek V., Elyashevich G.K. Percolation transitions in porous polyethylene and polypropylene films with lamellar structures. *Polymer Science, Ser. A*, 2015, **57** (6), P. 717–722.
- [11] Lee S.Y., Park S.Y., Song H.S. Lamellar crystalline structure of hard elastic HDPE films and its influence on microporous membrane formation. *Polymer*, 2006, **47** (10), P. 3540–3547.
- [12] Johnson M.B., Wilkes G.L. Microporous membranes of isotactic poly(4-methyl-1-pentene) from a melt-extrusion process. I. Effects of resin variables and extrusion conditions. *J. Appl. Polym. Sci.*, 2002, **83** (10), P. 2095–2113.
- [13] Xu J., Johnson M., Wilkes G.L. A tubular film extrusion of poly(vinylidene fluoride): structure/process/property behavior as a function of molecular weight. *Polymer*, 2004, **45** (15), P. 5327–5340.
- [14] Du C.H., Zhu B.K., Xu Y.Y. A study on the relationship between the crystal structure and hard elasticity of PVDF fibers. *Macromol. Mater. Eng.*, 2005, **290** (8), P. 786–791.
- [15] Dmitriev I.Yu., Bukošek V., Lavrentyev V.K., Elyashevich G.K. Structure and Deformational Behavior of Poly(vinylidene fluoride) Hard Elastic Films. *Acta Chimica Slovenica*, 2007, **54** (4), P. 784–791.
- [16] Sadeghi F., Tabatabaei S.H., Ajji A., Carreau P.J. Effect of PVDF Characteristics on Extruded Film Morphology and Porous Membranes Feasibility by Stretching. *Journal of Polymer Science: Part B: Polymer Physics*, 2009, **47** (12), P. 1219–1229.
- [17] Hu B., Cai Q., et al. Influence of uniaxial cold stretching followed by uniaxial hot stretching conditions on crystal transformation and microstructure in extrusion cast and annealed polyvinylidene fluoride porous membranes. *Journal of Plastic Film & Sheeting*, 2015, **31** (3), P. 269–285.
- [18] Ramadan K.S., Sameoto D., Evoy S. A review of piezoelectric polymers as functional materials for electromechanical transducers. *Smart Mater. Struct.*, 2014, **23** (3), Article ID 033001.
- [19] Wan C., Bowen C.R. Multiscale-structuring of polyvinylidene fluoride for energy harvesting: the impact of molecular-, micro- and macro-structure. *J. Mater. Chem. A*, 2017, **5** (7), P. 3091–3128.
- [20] Darestani M.T., Coster H.G.L., et al. Piezoelectric membranes for separation processes: Fabrication and piezoelectric properties. *Journal of Membrane Science*, 2013, **434**, P. 184–192.
- [21] Darestani M.T., Coster H.G.L., Chilcott T.C. Piezoelectric membranes for separation processes: Operating conditions and filtration performance. *Journal of Membrane Science*, 2013, **435**, P. 226–232.
- [22] Mao H., Qiu M., et al. Self-cleaning Piezoelectric Membrane for Oil-in-water Separation. *ACS Appl. Mater. Interfaces*, 2018, **10** (21), P. 18093–18103.
- [23] Bae J., Baek I., Choi H. Efficacy of piezoelectric electrospun nanofiber membrane for water treatment. *Chemical Engineering Journal*, 2017, **307**, P. 670–678.
- [24] Lu X., Guo Q., et al. Biosensor platform based on stress-improved piezoelectric membrane. *Sensors and Actuators A: Physical*, 2012, **179**, P. 32–38.
- [25] Xue X., Wang S., et al. Hybridizing Energy Conversion and Storage in a Mechanical-to-Electrochemical Process for Self-Charging Power Cell. *Nano Lett.*, 2012, **12** (9), P. 5048–5054.
- [26] Song R., Jin H., et al. A rectification-free piezo-supercapacitor with a polyvinylidene fluoride separator and functionalized carbon cloth electrodes. *J. Mater. Chem. A*, 2015, **3** (29), P. 14963–14970.
- [27] Ghosh S.K., Sinha T.K., et al. Porous polymer composite membrane based nanogenerator: A realization of self-powered wireless green energy source for smart electronics applications. *J. Appl. Phys.*, 2016, **120** (17), Article ID 174501.
- [28] Martins P., Lopes A.C., Lanceros-Mendez S. Electroactive phases of poly(vinylidene fluoride): Determination, processing and applications. *Progress in Polymer Science*, 2014, **39** (4), P. 683–706.
- [29] Dmitriev I.Yu., Kuryndin I.S., Lavrentyev V.K., Elyashevich G.K. Structure and Piezoelectric Properties of Microporous Polyvinylidene Fluoride Films. *Physics of the Solid State*, 2017, **59** (5), P. 1041–1046.
- [30] Chen D., Zhang J.X.J. Microporous polyvinylidene fluoride film with dense surface enables efficient piezoelectric conversion. *Appl. Phys. Lett.*, 2015, **106** (19), Article ID 193901.
- [31] Hermans P.H., Weidinger A. On the determination of the crystalline fraction of polyethylenes from X-ray diffraction. *Macromol. Chem.*, 1961, **44** (1), P. 24–36.
- [32] Nakamura K., Sawai D., et al. Effect of annealing on the structure and properties of poly(vinylidene fluoride) β -form films. *Journal of Polymer Science: Part B: Polymer Physics*, 2003, **41** (14), P. 1701–1712.
- [33] Amoresi R.A.C., Felix A.A., et al. Crystallinity, Morphology and High Dielectric Permittivity of NiO Nanosheets Filling Poly(vinylidene fluoride). *Ceramics International*, 2015, **41**, P. 14733–14739.
- [34] Haghiashtiani G., Greminger M.A. Fabrication, polarization, and characterization of PVDF matrix composites for integrated structural load sensing. *Smart Mater. Struct.*, 2015, **24**, Article ID 045038.
- [35] Elyashevich G.K., Kuryndin I.S., et al. Porous Structure, Permeability, and Mechanical Properties of Polyolefin Microporous Films. *Physics of the Solid State*, 2012, **54** (9), P. 1907–1916.
- [36] Stauffer D., Aharony A. *Introduction to Percolation Theory*, Taylor and Francis, London, 1994, 192 p.